



HAL
open science

Involvement of the Prion Protein in the Protection of the Human Bronchial Epithelial Barrier Against Oxidative Stress

Amal Kouadri, Mariam El Khatib, Johanna Cormenier, Sylvain Chauvet, Waël Zeinyeh, Micheline El Khoury, Laurence Macari, Pierre Richaud, Christelle Coraux, Isabelle Michaud-Soret, et al.

► **To cite this version:**

Amal Kouadri, Mariam El Khatib, Johanna Cormenier, Sylvain Chauvet, Waël Zeinyeh, et al.. Involvement of the Prion Protein in the Protection of the Human Bronchial Epithelial Barrier Against Oxidative Stress. *Antioxidants and Redox Signaling*, 2019, 31 (1), pp.59-74. 10.1089/ars.2018.7500 . hal-02092968

HAL Id: hal-02092968

<https://hal.science/hal-02092968v1>

Submitted on 22 Jun 2020

HAL is a multi-disciplinary open access archive for the deposit and dissemination of scientific research documents, whether they are published or not. The documents may come from teaching and research institutions in France or abroad, or from public or private research centers.

L'archive ouverte pluridisciplinaire **HAL**, est destinée au dépôt et à la diffusion de documents scientifiques de niveau recherche, publiés ou non, émanant des établissements d'enseignement et de recherche français ou étrangers, des laboratoires publics ou privés.

Original Research Communication

Involvement of the Prion Protein in the Protection of the Human Bronchial Epithelial Barrier against Oxidative Stress

Amal Kouadri¹, Mariam El Khatib¹, Johanna Cormenier¹, Sylvain Chauvet¹, Wael Zeinyeh¹,
Micheline El Khoury¹, Laurence Macari¹, Pierre Richaud³, Christelle Coraux⁴, Isabelle
Michaud-Soret¹, Nadia Alfaidy² and Mohamed Benharouga¹

¹ Univ. Grenoble Alpes, CNRS, UMR 5249, CEA, BIG, CBM, F-38000 Grenoble, France.

² Univ. Grenoble Alpes, INSERM U1036, CEA, BIG, BCI, F-38000 Grenoble, France.

³ Univ. Aix-Marseille, CNRS, CEA, Institut de Biosciences et Biotechnologies d'Aix-Marseille (BIAM), UMR 7265, CEA Cadarache, Saint-Paul-lez Durance F-13108, France.

⁴ Institut National de la Santé et de la Recherche Médicale (INSERM), UMR-S 903, Reims, France.

Running Title: Role of PrP^C protein in the lung epithelial barrier.

Keywords: Prion protein, Bronchial epithelium, Oxidative stress, Copper, Junctional proteins

Address correspondence to:

Dr. Mohamed Benharouga

LCBM-UMR5249

DRF-BIG, CEA-Grenoble

17 rue des Martyrs, F-38054, Grenoble cedex 09, France

Téléphone: (33)-4-38-78-44-51

Fax: (33)-4-38-78-54-87

E-mail: mohamed.benharouga@cea.fr

Word count: 6106

Reference numbers: 73

Greyscale illustrations: 7

Color illustrations: 3 (online 3)

Abstract

Aim: Bronchial epithelium acts as a defensive barrier against inhaled pollutants and microorganisms. This barrier is often compromised in inflammatory airway diseases that are characterized by excessive oxidative stress responses, leading to bronchial epithelial shedding, barrier failure, and increased bronchial epithelium permeability. Among proteins expressed in the junctional barrier and participating to the regulation of the response to oxidative and to environmental stresses is the cellular prion protein (PrP^C). However, the role of PrP^C is still unknown in the bronchial epithelium. Herein, we investigated the cellular mechanisms by which PrP^C protein participates into the junctional complexes formation, regulation, and oxidative protection in human bronchial epithelium.

Results: Both PrP^C mRNA and mature protein were expressed in human epithelial bronchial cells. PrP^C was localized in the apical domain and became lateral, at high degree of cell polarization, where it co-localized and interacted with adherens (E-cadherin/ γ -catenin) and desmosomal (desmoglein/desmoplakin) junctional proteins. No interaction was detected with tight junction proteins. Disruption of such interactions induced the loss of the epithelial barrier. Moreover, we demonstrated that PrP^C protection against copper associated oxidative stress was involved in multiple processes, including the stability of adherens and desmosomal junctional proteins.

Innovation: PrP^C is a pivotal protein in the protection against oxidative stress that is associated with the degradation of adherens and desmosomal junctional proteins.

Conclusion: Altogether, these results demonstrate that the loss of the integrity of the epithelial barrier by oxidative stress is attenuated by the activation of PrP^C expression, which deregulation might be associated to respiratory diseases.

Introduction

The bronchial epithelium forms a critical barrier that is continually exposed to a variety of environmental agents such as pollutants, allergens, particles and microorganisms that are capable of causing tissue injury. These injuries are normally countered by the establishment of an effective line of defense and repair mechanisms (51,65). The periciliary surface fluid and mucus form the first line of defense of the airways, including the production of abundant mediators and innate airway immune responses (31). The second line is physical and consists of three main types of intercellular junctional complexes responsible for the sealing of the epithelium: tight junctions, adherens junctions and desmosomes (25,31,34). The disruption of the intercellular junction of bronchial epithelium is associated with an increase in epithelial cell permeability and an invasion by infectious agents (37,42,69). This phenomenon constitutes a hallmark of inflammatory and chronic infectious diseases, such as cystic fibrosis (CF) (10). One of the parameters that was reported to contribute to the airway epithelial barrier's injury and dysfunction is the oxidative stress status, induced by endogenous productions of reactive oxygen species (ROS) (26,39,47). To protect and repair the injured epithelial barrier following exposure to an oxidative stress, the cells setup an anti-oxidative system that involves molecules such as vitamins E and C, with the ability to scavenger intracellular free radicals; peptides such as glutathione that chelate free copper; and enzymes such as catalase and superoxide dismutase (SOD) (45,68).

The cellular prion protein (PrP^{C}) is one of the proteins that have been reported to be involved both in antioxidant protection (1,33) and in maintaining the integrity of the intestinal epithelial barrier (49,54). PrP^{C} is a glycosyl phosphatidyl inositol (GPI)-anchored glycoprotein known for its unique ability to undergo structural conversion from a normal isoform (PrP^{C}) into a pathogenic conformer known as scrapie (PrP^{Sc}) (57). The accumulation of PrP^{Sc} aggregates in the brain is a distinctive feature of transmissible spongiform encephalopathies (TSE), a group of animal and human lethal neurodegenerative diseases (14). The physiological role of the cellular PrP has mainly been associated with stress-protection (60,73), copper homeostasis (2) and neuronal excitability (38). Other functions related to cellular processes and metabolism have also been reported for this protein (11). In epithelial cells, PrP^{C} localization is still a matter of

discussion and the majority of data were obtained in enterocytes and MDCK cells (18,44,49,50,52,62,67). In these cells, PrP^C was reported to be directed to the apical and/or basolateral membranes (18,44,49,50,52,62,67).

Recently, in a fully polarized MDCK cells, a basolateral to apical transcytosis was also reported for the full-length PrP^C and its fragments of cleavage (3). However, in highly polarized enterocytes PrP^C was found to be targeted to the lateral junctional complexes of adjacent cells and to interact with junctional proteins (3,62).

To date, the role of the PrP^C in the oxidative stress protection and in copper homeostasis in epithelial cells, including bronchial epithelial cells, is still poorly documented and the link between its protective function and its localization in the apical and/or basolateral domains of bronchial epithelial cells is still unknown.

We used the human bronchial epithelial cells (16HBE14o-) as a model (21) to investigate the expression, localization, regulation and function of PrP^C in relation to oxidative stress and copper status. We demonstrated that PrP^C protein i) is expressed at the apical and basolateral sides ii) undergoes apical-to-basolateral transcytosis in fully polarized 16HBE14o- cells, iii) localizes and interacts with adherens junction proteins, vi) impacts cell-cell adhesion and cell junctions' integrity. More importantly, we demonstrated that PrP^C is involved in copper homeostasis and in the protection against the collapse of the bronchial epithelial barrier caused by oxidative stress.

Altogether, this study highlights, for the first time, the role of PrP^C protein in the protection of the lung barrier against oxidative stress by increasing its proper expression and by stabilizing key junctional proteins. These findings will improve our understanding of the oxidative stress-associated with the loss of the integrity of the epithelial barrier in inflammatory and chronic infectious lung diseases.

Results

PrP^C expression and characterization in human bronchial epithelial cells

The expression of PrP^C protein was examined in human pulmonary epithelial cells. We used a well-established transformed bronchial epithelial cell line 16HBE-14o- (HBE) (16) that was kindly provided by Dr. D.C. Gruenert (University of California, CA) and A549, a human lung adenocarcinoma epithelial cell line. These cells are widely used as *in vitro* models to study type II pulmonary epithelial cells (ATCC, (23)). Both cell lines are able to grow as adherent

monolayer cells by developing cell-cell interactions through junctional complexes. However, only HBE cells are able to develop a progressive and high trans-epithelial resistance (TER). In our conditions, A549 reached a maximum TER-value of approximately $18 \Omega/\text{cm}^2$ after 9 days of culture, while HBE cells developed a TER of $\sim 650 \Omega/\text{cm}^2$ (Fig. S1-A). Comparable TER-values have been reported previously (22). These findings confirm that despite normal distribution of junctional barrier proteins in the both cell types, A549 cells are not able to develop comparable tightness to HBE cells. This makes HBE cells a good model to study the role of proteins that are involved in the development and the maintenance of intercellular junctions.

Using RT-PCR, we demonstrated that PrP^C gene is expressed in HBE and A549 cells (Fig. 1A). As control, we used N2a, mouse neuroblastoma cells commonly used to study PrP^C (24,41,56), and *HTR-8/SVneo cells*, a human anchoring trophoblast cell line, in which PrP^C expression has previously been characterized (2). PrP^C mRNA was highly expressed in HBE compared to A549 and N2a cells (Fig.1B). These results were confirmed by immunoblot assay (Fig. 1C). The anti-PrP antibodies recognized three different PrP^C forms in HTR, N2a, A549 and HBE cells. These forms correspond to the unglycosylated (~ 24 kDa), the immature glycosylated ($\sim 26-30$ kDa), and the mature highly glycosylated PrP^C ($\sim 31-37$ kDa) (Fig. 1C). The level of expression was evaluated using Na⁺/K⁺-ATPase α -subunit as loading control. Similar results were obtained using a second loading control, the β -actin (Fig. S1-B).

At the cellular level, PrP^C maturation is characterized by its degree of glycosylation and by its expression at the plasma membrane (30). As previously described (18), the glycosylation of mature PrP^C was sensitive to N-glycosidase F (F) and insensitive to endoglycosidase H (H), indicating the expression of mature PrP^C in A549 and HBE cells (Fig.1D).

To further characterize PrP^C expression, we analyzed its digestion profile using the proteinase K (PK) enzyme. It is well established that only PrP^{SC} is resistant to PK, while PrP^C is completely digested (9). Our results showed that the PrP^C protein expressed in HBE and A549 cells were totally digested by PK (Fig. 1E), indicating that the PrP^C protein detected in lung epithelial cells exhibits a normal conformation.

Human tissue and cellular localization of PrP^C

To characterize the localization of PrP^C protein in human bronchial epithelial cells and to analyze the tissue distribution in human bronchi, we performed both immunohistochemical and immunofluorescence analyses using human healthy lung sections (Fig. 2A) and fixed A549 and HBE cells (Fig. 2B-E).

At the tissue level, PrP^C protein was mainly detected in cilia cells in which the localization appeared to be cytoplasmic and at the plasma membrane, mostly at the lateral and apical sides (Fig. 2A (c)). Low expression was observed in the connective tissue (Fig. 2A (c)). Incubation in the absence of the primary antibody (Fig. 2A (a)), or in the presence of the primary antibody (SAF32) that has been preincubated overnight with the immunogen peptide (Fig. 2A (b)) confirmed the specificity of PrP^C detection at the bronchial level.

For the cellular localization, we used immunofluorescence cell imaging and X/Z image reconstitution to analyze the distribution of PrP^C in exponentially growing (3 days of culture) or in polarized (10 days of culture) A549 and HBE cells. When A549 and HBE cells were used before the establishment of a cell-cell junction (3 days), PrP^C protein was detected at the apical, lateral and in the cytoplasmic domains (Fig. 2B and 2C). Interestingly, in confluent and polarized cells (10 days), only HBE cells that developed a high TER (Fig. S1-A) exhibited a unique lateral localization of PrP^C (Fig. 2D and 2E), while A549 cells, even after 10 days of culture, did not display any change in the PrP^C distribution, compared to those observed after 3 days of culture (Fig. 2B and 2C).

Altogether these results reveal that PrP^C distribution in HBE cells is dependent upon the cell polarization, highlighting its potential role in the maintenance and/or control of the cell's junction repertoire.

PrP^C colocalizes with key junctional proteins

Since the immunolocalization results showed that PrP^C was localized to the lateral membrane of polarized HBE cells (Fig. 2), we investigated the co-localization profiles of PrP^C with different junctional resident proteins using immunofluorescence imaging cells, combined with X/Z image reconstitution. PrP^C was found to co-localize with γ -catenin and E-cadherin, two representative proteins of the adherens junctions (Fig. 3A and 3B). PrP^C also co-localized with desmoplakin and desmoglein, two proteins of the desmosome junctions (Fig. 3A and 3B).

However, no co-localization was found with ZO-1 protein, a member of the tight junctions (Fig. 3A and 3B). In A549 cells, PrP^C protein also co-localized with E-cadherin, γ -catenin, and desmoplakin (Fig. S1-C and S1-D).

Because it was reported that PrP^C protein could also be localized into the nucleus of intestinal cells (7), we searched for such localization in the HBE cells. Very light staining was observed in the nucleus of HBE cells, suggesting a possible nuclear localization of PrP^C protein in this cell type. To verify the existence of such localization, we performed a nucleus staining using DAPI (4',6-diamidino-2-phenylindole), a fluorescent stain that binds strongly to DNA; anti-Ki-67, a nucleus resident protein that is associated with cell proliferation; and an anti-PrP^C antibody. Figure 3C shows that Ki-67 and DAPI co-localized in the nucleus. However, no staining and/or colocalization was found with the PrP^C protein (Fig. 3C), suggesting that the localization and the role of PrP^C in lung bronchial epithelial cells are restricted to the plasma membrane.

PrP^C interacts with junction-associated proteins and is involved in the maintenance of the junctional barrier

The co-localization results suggested that PrP^C protein might interact with junction-associated proteins. To verify this hypothesis, we immunoprecipitated PrP^C protein using an anti-PrP^C specific antibody (SAF-32). The targeted proteins were detected using western-blot analysis. We demonstrated that PrP^C does not interact with ZO-1 (Fig. 4A). However, PrP^C interacts with γ -catenin, E-cadherin, desmoplakin and desmoglein (Fig. 4A). To confirm the specificity of the antibody-antigen interaction, we used a non-specific antibody (mAb0) instead of the SAF-32 antibody to immunoprecipitate the PrP^C protein. The results reported in figure S2-A confirm the specificity of SAF-32 for the PrP^C protein. These results suggest the involvement of PrP^C in the establishment of the junctional complexes in the bronchial epithelial tissue.

To test this hypothesis, we knocked down PrP^C expression using siRNA strategy, and measured the TER and fluorescein-5-isothiocyanate (FITC)-inulin transport. To invalidate the PrP^C expression in HBE cells, we tested two different siRNA labelled #1 and #2. Both siRNA knocked down PrP^C expression at mRNA and protein levels, as reported in figure S2-B-D. For the subsequent experiments using siRNA strategy, only siRNA#1 was used.

The TER was assessed during 8 days of culture to determine junction formation and strength (Fig. 4B). TER levels at days 8 of culture were plotted in figure 4C. As expected, TER increased in a time-dependent manner and reached a plateau after 8 days of culture ($\sim 620 \Omega \cdot \text{cm}^2$), which reflects the formation of cell-cell junctions (Fig. 4B and 4C). Interestingly, in PrP^C-knockdown HBE cells the TER levels were lower ($\sim 50\%$, $\sim 300 \Omega \cdot \text{cm}^2$) compared to the control condition (Fig. 4B and 4C). In addition to TER results, the evaluation of the transport of FITC-inulin demonstrate the increase of the paracellular permeability upon PrP^C knock down in HBE cells (Fig. 4D). Thus, the decrease in TER associated with enhanced permeability to inulin is an indicator of loss of bronchial epithelial barrier function.

Altogether, these results demonstrate for the first time, the direct involvement of PrP^C protein in the junction formation of bronchial epithelial cells.

Cu upregulates PrP^C expression in human bronchial epithelial cells and in mice bronchial epithelial tissue

Since PrP^C protein binds with high affinity 5 copper ions (8), we first analyzed the dose and time-dependent effects of Cu on PrP^C expression in HBE cells. After Cu stimulation, PrP^C expression gradually increased in a concentration- (Fig. 5A and 5B) and time-dependent manners (Fig. 5D).

PrP^C protein levels were quantified and normalized based on the levels of the alpha subunit of Na⁺/K⁺-ATPase (Fig. 5B). As shown in Fig. 5A, PrP^C was detected in untreated HBE cells as U-, I- and H-glycosylated forms. Following Cu stimulation, the three glycosylated forms gradually increased after 24h of treatment (Fig. 5A and 5B). Similar to PrP^C protein expression, the PrP^C mRNA levels were also significantly increased in response to Cu treatment (Fig. 5C and 5E), suggesting a transcriptional effect. Using a non-epithelial N2a cells, we observed that copper treatment also increased the expression of the three forms of PrP^C protein (Fig S3-A and B).

The high level of the H-glycosylated form of PrP^C observed following Cu treatment suggested an increase of PrP^C insertion into the plasma membrane. This hypothesis was confirmed by the cell surface biotinylation assay (Fig. 6A). Image analysis revealed that, compared to the control condition (absence of Cu), the abundance of biotinylated PrP^C

was increased ~25% following 24h of Cu-treatment (100 μ M), suggesting that the H-glycosylated form is almost totally inserted into the plasma membrane (Fig. 6B).

Cu increases PrP^C expression, specifically at the junctional side of HBE cells

To determine the HBE cells membrane domain (apical, lateral and/or basolateral) in which the H-form of PrP^C protein was expressed following Cu treatment (Fig. 6A and B), we used immunofluorescent assays (Fig. 6C and 6D). Following Cu treatment, we observed an increase in PrP^C expression in non- and in permeabilized HBE cells (Fig. 6C, X/Y). The X/Z image reconstitution (Fig. 6C, X/Z) demonstrates that the plasma membrane fluorescence increased specifically in the lateral side. The quantification of the intensity of the lateral fluorescence indicated an increase of ~65% and ~40% in non- and in permeabilized HBE cells, respectively (Fig. 6D), suggesting that PrP^C insertion at the lateral side might play an important role in the protection of the junctional barrier against the effects of oxidative stress in bronchial epithelial cells.

To get more insights into the effect of copper on PrP^C expression in an *in vivo* system, we evaluated the effect of copper treatment on PrP^C expression in bronchial epithelial tissue, by watering 8-10 weeks C57BL/6 mice with aquatic solution containing copper. The efficiency of Cu treatment was determined by the measurement of blood Cu concentrations as previously reported by our group (2).

Immunohistochemistry analysis of lung tissues collected from control and copper treated mice showed that PrP^C was expressed in ciliated and basal cells in control mice (Fig. S3-B (b) and (c)). Following copper treatment, the PrP^C expression increased in bronchial tissues (Fig. S-B (c)). Altogether, these results suggest that there might be a strong relationship between the concentration of extracellular copper and the levels of PrP^C expression in the bronchial epithelial tissue.

Elevated PrP^C levels protect against Cu accumulation, Cu-induced oxidative stress production, and bronchial epithelial cell death

Copper homeostasis is finely regulated and any disruption of its physiological concentrations causes an increase in the intracellular oxidative stress. The increase in PrP^C expression upon Cu treatment may reveal a stress protective response within the cell. To test the role of elevated PrP^C expression in preventing the Cu-induced cytotoxicity, we first measured the HBE cells viability using the MTT assay. After 24 h of incubation with the

indicated Cu concentrations, HBE cells exhibited a significant cell death of ~30% at 100 μM (Fig. 7A). Similar degree of cell death was observed at 200 μM (Fig. 7A).

Based on the high proportion of dead cells, we hypothesized that this might be the consequence of an oxidative stress induced by the increase in the intracellular copper concentrations. Using ICP-AES assay, we confirmed that the intracellular concentrations of Cu increased in a dose-dependent manner (Fig. 7B). To confirm the relationship between copper and the levels of PrP^C expression, we knocked down the cellular prion protein using siRNA strategy. Knockdown of PrP^C had no significant effect on cell survival (Fig. 7C). A significant increase in cell death was however observed in PrP-depleted HBE cells (~80% at 24h) following incubation with 100 μM of Cu (Fig. 7C).

Then we monitored the oxidative-stress production and intracellular Cu content following Cu treatment in the absence or presence of PrP^C. After exposure of HBE cells to 100 μM of Cu, the DCF fluorescence, indicative of the presence of an oxidative stress, increased compared to untreated HBE cells (Fig. 7D). In the PrP^C-silenced HBE cells, the level of DCF fluorescence was similar compared to the control HBE (Fig. 7D). The treatment of PrP-knockdown HBE with 100 μM of Cu increased the oxidative stress accumulation by ~2-fold (Fig. 7D).

Finally, using PrP-knockdown HBE cells we confirmed that PrP^C participates into the regulation of the intracellular Cu concentration (Fig. 7E). Using ICP-AES we found that Cu concentration in normal HBE was ~0.02 $\mu\text{g}/10^6$ cells (Fig. 7E). A slightly elevated copper levels (~0.03 $\mu\text{g}/10^6$ cell) were observed in PrP^C-silenced HBE cells (Fig. 7E). When Cu was added during 24h, the intracellular copper concentration was increased to ~0.8 $\mu\text{g}/10^6$ cell in wild type and to ~1.3 $\mu\text{g}/10^6$ cell in PrP^C-depleted HBE, respectively (Fig. 7E).

ROS-mediated increase of PrP^C in HBE cells

Based on the results reported in figures 5A and 7D, 24h of treatment with 100 μM of copper significantly increased PrP^C expression and the production of pro-oxidants molecules in HBE cells. These data suggested that PrP^C increased expression might in part be due to a primary increase in pro-oxidants molecules, such as hydrogen peroxide (H_2O_2). This hypothesis was tested by treating HBE cells for 24h with 100 μM of H_2O_2 in the absence or in the presence of 100 μM of Trolox, a hydrophilic analogue of vitamin E (Vit E) that acts as a free radicals scavenger (63).

First, we evaluated the ability of Vit E to reduce the intracellular level of ROS in HBE cells. As shown in figure 8A, treatment with H₂O₂ significantly increased the levels of ROS that were reduced in the presence of Vit E. Interestingly, the invalidation of PrP gene expression led to the collapse of the antioxidant protection provided by the PrP^C protein, as demonstrated by the elevated levels of ROS in the presence of H₂O₂ and by their reduction in the presence of the Vit E (Fig. 8A). To confirm our results, we performed an immunoblot using proteins extracts prepared from HBE cells treated for 24h either with copper (Cu), Vit E, H₂O₂, or Vit E plus H₂O₂ (H₂O₂+Vit E). Treatment with 50 μM of copper increased the expression of PrP^C protein. Similar results were observed upon treatment with H₂O₂, however, only the expression of the U- form was increased (Fig. 8B). The H- and I- forms appeared to slightly decrease compared to the control condition (Fig. 8B). Similar data were observed in neuronal cells and have been reported to result from PrP^C cleavage at the end of the copper-binding octapeptide repeats through the action of ROS, a process termed β-cleavage (71).

To further clarify the relationship between PrP^C expression and ROS production, we evaluated the effect of iron (Fe), a metal known to exhibit less affinity for PrP^C compare to copper and known to be a source of ROS production via the Fenton reaction (72). Treatment of HBE cells during 24h with the iron induced an increase in the expression of H- and I- PrP^C forms and to less extent the U-form (Fig. 8C). Altogether, these results demonstrate that PrP^C protein responds to oxidant aggressions independently of their origin.

Copper induced PrP^C expression is mainly transcriptional.

Since we showed that copper treatment increases the production of oxidative stress (Fig. 7D) and that ROS production increased PrP^C expression (Fig. 8B), we performed different experiments to evaluate the effect of copper associated oxidative stress on PrP^C expression. First, we demonstrated that Trolox treatment is able to reduce ROS levels, produced after treatment with copper (Fig 9A). Compared to the control condition (Fig. 9B), Trolox treatment did not affect the levels of PrP^C expression following copper treatment (Fig. 9 C), demonstrating that even in the absence of any oxidative stress, copper treatment still increases the levels of PrP^C protein expression. Similar results have been observed at the level of the mRNA, using Trolox (Fig. 9D). Our results demonstrate

that copper increases the expression of PrP^C through the Cu-associated oxidative stress but also through a transcriptional pathway. However, the latter is more predominant as previously reported in placental cells (2).

PrP^C protein protects the junctional proteins against Cu oxidative effects

The functional effects of Cu on the permeability of the junctional barrier in polarized HBE cells were monitored by measuring TER values upon their treatment with 100 μM of Cu, from the apical side, for the indicated times. As shown in Fig. 10A, copper ions decreased TER values in a time-dependent manner, as evidenced by the decrease in TER values (~20%) (Fig. 10B). The levels of TER measured in the HBE cells treated with copper were compared to those obtained in PrP^C-knockdown HBE cells (Fig. 10B), at day 4 of confluence.

The results indicated that in HBE cells the decrease in PrP^C expression (siPrP^C) increased cell permeability (~50%) compared to Cu treatment (~18%). Our results suggest that the increase in PrP^C expression in the lateral side of bronchial epithelial cells (Fig. 6) protects the junctional barrier against the Cu-inducing oxidative stress that might affect the levels of expression of junctional protein, as was previously reported (20).

To test our hypothesis, we first evaluated the effect of copper treatment on the steady state expression of tight junctions (ZO-1, occluding (Occ)), adherents (γ-catenin (γ-Cat) and E-cadherin (E-Cad)) and desmosome (desmoplakin (Dep)) junctions. The results showed that in the presence of copper only ZO-1 expression decreased in a time-dependent manner (Fig. 10C). Neither γ-Cat/E-Cad nor desmoplakin proteins were affected by the copper treatment (Fig. 10C).

Subsequently, we assessed the stability of ZO-1 and occludin proteins using cycloheximide (CHX) assays in the absence or in the presence of copper. As reported in figure 10D the degradation of ZO-1 and occludin (Occ) were accelerated in the presence of copper.

Using PrP^C-knockdown HBE cells, we evaluated the role of PrP^C protein using cycloheximide (CHX) assays in the absence or in the presence of copper (Fig. 10E).

Since there was no co-localization, or interaction between PrP^C and ZO-1 protein (Fig. 3 and 4), we were not surprised to observe that the degradation rate of ZO-1 was not accelerated in PrP^C-knockdown HBE cells, in the absence or in the presence of copper (Fig. 10E). Unexpectedly, occludin degradation was accelerated under the same conditions,

suggesting that ZO-1 and occludin are differentially regulated by PrP^C and copper, although they belong to the same family of tight junctions. The degradation rate of desmoplakin (Dep) and desmoglein (Deg), proteins that interact with PrP^C, was significantly increased in PrP^C-knockdown HBE cells, particularly in the presence of copper (Fig. 10E). Similar results were obtained using a second siRNA (siPrP (#2)) (Fig. S4-B) compared to the control, using scrambled siRNA (Fig. S4-A).

These results demonstrate that by interacting and stabilizing the junctional proteins (adherens and desmosomes), PrP^C participates in the oxidative stress protection and in the maintenance of the bronchial epithelial junctional barrier.

Discussion

The present study is the first to demonstrate that PrP^C is expressed in the human bronchial epithelial cells, which form a physical barrier to inhaled toxic particles, bacteria and viruses (58). Using multiple approaches, we provide strong evidences for a novel role of the PrP^C protein in the protection of the bronchial epithelial barrier against potentially generated oxidative stress. The *in vivo* studies performed both in mice and human demonstrated that the PrP^C protein is highly expressed in the bronchial epithelial cells, comforting the search of its role in this epithelium.

Importantly, we demonstrate that PrP^C expression, glycosylation and digestion profiles detected in A549 and HBE cell lines were similar to those reported in intestinal epithelial cells (49), (50) and placental trophoblast cells (2). Moreover, the amount of PrP^C protein was 4 and 5 times higher in human HBE cells compared to human (SH-SY5Y) and mice (N2a) neuronal cells (data not shown), suggesting an important role for PrP^C in the bronchial epithelium function.

Compared to renal and intestinal MDCK and Caco-2 epithelial cells (18,49), HBE cells display also a high number of *PrP* gene copies and a high levels of PrP^C protein.

HTR, A549 and HBE cell lines mostly expressed PrP^C forms of lower electrophoretic mobility with apparent molecular weights between 30 and 37 kDa, compared to N2a cells that exhibit 26-30 kDa molecular weights for the PrP^C. Similar results were previously reported in N2a cells when compared to the rat B104 neuroblastoma, the mouse hypothalamic GT1-7, and the rat adrenal pheochromocytoma PC-12 cell lines (48). Monnet

et al (48) reported that in N2a cells the threshold of detection of the PrP^C was too low to evaluate the distribution of its multiple forms.

Although the molecular difference between the glycosylated forms in N2a and the other cells types is still to be elucidated, the deglycosylation results clearly showed that the 30-37 kDa PrP^C forms detected in HTR, A549 and HBE cells correspond to the PrP^C forms observed in N2a cells. The N-glycosylated forms of PrP^C might exhibit different glycan chains or derivatizations depending on the cell type. PrP^C deglycosylation in the different cell extracts including N2a cells (Fig. S4-C) indicated that the glycosylation processes were similar for all samples. The cellular prion protein glycosylation and expression levels may vary depending on the cell's density and/or state of differentiation, as previously reported for neuroblastoma B104 cells (48). Other possibility is that PrP^C protein may undergo proteolytic processing resulting in the production of different fragments as previously reported (40). In our study, copper-dependent β -cleavage is certainly taking place. The β -cleavage performed by radicals in a Fenton type reaction has been proposed to take place around the amino acid position, 90 of the PrP^C protein (40). In consequence of this cleavage, an N-terminal fragment of ~9 kDa (termed N2) is released whereas a corresponding C2 fragment of 18–20 kDa (depending on the glycosylation status) remains bound to the cellular membrane. To avoid the interference of this parameter with the interpretation of our results regarding the expression of the full length PrP^C protein under its different glycosylation states, we used the SAF-32 mAb that recognizes the whole octarepeated region of PrP^C spanning residues 51-98 (28).

To date, there is no consensus regarding the precise localization of the PrP^C in epithelia. Several groups, including ours, have proposed an apical localization of PrP^C in MDCK cells (13,18,59), which diverge from other studies showing a baso-lateral localization (62,67). These findings suggest that PrP^C localization is either controlled by the degree of epithelial cell polarization or that the PrP^C protein contributes to epithelial cell fusion and polarization. Such transcytosis trafficking has been recently observed in polarized epithelial MDCK cells (3).

PrP^C was detected in junctional complexes of the lateral membranes of adjacent polarized HBE cells where it was found to co-localize and interact with E-cadherin and desmoglein, and with their cytoplasmic partner, γ -catenin (plakoglobin) and desmoplakin. Interestingly,

no co-localization or interaction of PrP^C was reported with tight junction proteins. Similar results were described in enterocytes, where PrP^C was reported to be targeted to cell–cell junctional zone and to interact with several desmosomal (desmoglein-2, desmoplakin, γ -catenin), but not with adherens proteins (49). The absence of interaction with E-cadherin in enterocytes cells, even if a cellular co-localization was observed (49), suggested that in the bronchial epithelium such interactions might be important for the stability and the function of the junctional barrier.

In relation to the intracellular localization of PrP^C, it was reported that this protein could also be localized into the nucleus of intestinal cells (7). Based on the primary structure of the PrP protein and the site of its biosynthesis and maturation (64), the corresponding sialoglycoprotein is normally addressed to the plasma membrane where it can be released by phospholipase or protease treatments (64). Importantly, in the mouse scrapie-infected neuroblastoma cell line (ScN2a), immunocytochemical studies revealed that PrP^{Sc} and/or PrP^C are present, not only at the plasma membrane or in cytoplasmic compartments (12,43), but also in the nuclear compartment, particularly into the nucleolus (55).

According to its size (24 to 37 kDa), PrP^C is able to enter the nucleus either in an energy-dependent pathway if it possesses an NLS or by passive diffusion. Indeed, the analysis of the primary structure of the mature protein have revealed the existence of a nuclear localization sequence in N-terminal extremity (KKRPKP noted Pnls) (6,27). Through our experiments, we cannot conclude that PrP^C protein is localized into the nucleus of HBE cells. This statement is based on the co-immunofluorescence experiments that did not show any co-localisation between the PrP^C and Ki-67. Interestingly, as reported for trophoblast cells (2), the incubation of HBE cells with Cu increased PrP^C plasma membrane insertion, providing evidences for a potential role of PrP^C as a Cu sensor and/or chelator at the cell surface to protect these cells from Cu excess. However, in neurons, it has been reported that treatment with Cu increased PrP^C endocytosis (53), suggesting that the role of PrP^C protein in copper homeostasis is cell-dependent. Importantly, our *in vivo* approach substantiated the increase of PrP^C expression at the bronchial level, upon Cu intake by the mice. Because of the immediate endocytosis of PrP^C protein upon copper binding, one can speculate that prion protein could constitute a real copper transporter. In fact, once PrP^C binds extracellular copper on the cell surface and, when endocytosed and exposed to

lower pH of intracellular organelles, releases the metal ions. This hypothesis is very tempting, however multiple biochemical studies rather support the sensor role of PrP^C for copper and for other metals such as Zn²⁺ and Mn²⁺ (35,46,70).

The increase in PrP^C expression following Cu treatment caused a significant increase in the intracellular Cu concentration, along with an increase in ROS production. In addition, the loss of the expression of PrP^C protein, in the presence of Cu, caused dramatic effects on HBE viability and increased Cu content and ROS production. These finding highlights the stress protective role of PrP^C protein in bronchial epithelial cells and substantiate recent publish data reporting a stress protective role of PrP^C protein (60,73). We also confirm that PrP^C protein respond to other type of stress such as H₂O₂ and iron. Regarding iron, recent reports also indicated that PrP^C promotes cellular iron uptake by functioning as a ferrireductase (29). However, the metal transporter(s) involved in PrP^C-associated iron uptake and transport are not known. Human neuroblastoma cells (M17) that over-express PrP^C show resistance to higher amounts of ferric ammonium citrate (FAC) relative to non-transfected cells, suggesting a dose-dependent protection against redox-iron. One likely explanation for these observations is that interaction of redox-iron with copper and iron bound PrP initiates the Fenton reaction, resulting in denaturation and aggregation of PrP at the cell surface (17).

In addition, we demonstrated that even if PrP^C expression is increased during oxidative stress, under copper treatment, its levels of expression are mainly controlled through a transcriptional pathway.

However, the link between the role of PrP^C in bronchial epithelial barrier and its associated role against the oxidative stress is still to be demonstrate.

One of the consequences of chronic oxidative stress in the lung is the bronchial epithelial shedding and the breakdown of epithelium cohesion (4,5,36). Several reports in the literature have shown that damages caused by free radicals in epithelial cells are associated with an increase in the tight junction's permeability (4,5,61). We confirmed this finding in HBE cells and further demonstrate that these effects were ZO-1 and occluding dependent. Similar results have been reported in Caco-2 cells (19,20). The *PrP* gene invalidation in HBE cells caused a decrease in TER along with an increase in the instability

of tight and desmosomal protein junctions, highlighting the importance of PrP^C protein in oxidative protection of junctional proteins.

Through its interactions, PrP^C protein might ensure the stability and an oxidative stress protection for E-cadherin, γ -catenin, desmoplakin and desmoglein. The absence of such interactions might lead to the degradation of key junctional proteins, as was observed for ZO-1 and occludin. Previous studies, reported that in Caco-2 cells copper induced a concentration- and time-dependent decreases in the expression of tight junction proteins along with an increase in their permeability (19,20). These effects might be explained by the absence of interactions between PrP^C and E-cadherin, as previously reported in these cells (49).

Altogether our results demonstrate that PrP^C protein by forming complexes with E-cadherin/ γ -catenin and desmoglein/plakoglobin proteins participates in the regulation, the stability and the oxidative protection of adherens and desmosomal junctions in the bronchial cell barrier. Yet, it is still to be demonstrated whether the induction of PrP^C expression and its lateral localization are protective mechanisms during chronic airway diseases.

Innovation:

Chronic bronchial infection, inflammation and oxidative stress in pulmonary diseases such as cystic fibrosis lead to epithelial cell disorganization along with increased permeability. Yet, the mechanism by which this occurs is still to be determined. Here we brought evidences that the cellular prion is involved in the protection of the bronchial epithelial barrier upon oxidative stress occurrence. PrP^C protection of the lung epithelial barrier was exhibited through its capacity to interact and to stabilize adherens and desmosomal protein.

Experimental Procedures

Human tissues collection

Peripheral human lung tissue (containing non cartilaginous airways) was obtained at the time of lung transplantation from non-smoking controls undergoing lung resection upon peripheral lung cancer (Grenoble Hospital). Lung tissue samples were fixed in 10% neutral buffered formalin by inflation-immersion and embedded in paraffin. Collection and

processing of human lungs were conformed to the declaration of Helsinki and to all the rules of the local Committees on Human Research. Informed consent was obtained from each patient.

Mice tissues collection

For the *in vivo* experiments, mice (8–10-weeks old, 20–25 g) of C57BL/6 strains were used. Mice were obtained from the animal facility of CNRS (Orléans, France). The mice were randomly assigned to receive either distilled water, containing 50 ppm sucrose, or 250 ppm copper (copper sulfate (CuSO₄)) and 50 ppm sucrose.

All procedures involving animals and their care were approved by the local institutional Ethics Committee. Mice were sacrificed using cervical dislocation after chloral hydrate anesthesia. Fresh lungs were collected from each animal. Shortly after collection, tissues were fixed in 4% paraformaldehyde at room temperature.

Immunohistochemistry

5 µm paraffin-embedded sections were prepared from human non-smoking peripheral lung tissues. Immunohistochemistry was performed as described previously (2). Sections were incubated with anti-PrP antibody (SAF32, Bertin-Pharma, France). Immunopositive staining was detected using a Vectastain ABC kit (Vector Labs) using DAB (3, 3'-diaminobenzidine) as the chromagen (Vector Labs). Slides were counterstained using hematoxylin (Sigma Aldrich, France). Control sections were treated with either the secondary antibody alone or with the anti-PrP^C antibody (SAF-32) that has been preabsorbed overnight at 4°C with the appropriate antigen peptide (Covalab company, Lyon, France).

Immunohistochemistry was also performed on lung sections collected from C57 mice as described previously (2).

Cell culture

All culture media were purchased from Life-Technologies (France). The mouse neuroblastoma (N2a) and adenocarcinoma human alveolar basal epithelial (A549) cell lines were cultured in high glucose DMEM-Glutamax (Dulbecco's Modified Eagle's Medium) medium, whereas HBE cells were cultured in normal MEM (Modified Eagle's Medium) medium.

All media were supplemented with 10% fetal Bovine serum (Biowest, France) and 1% antibiotics mix (100 IU/ml of penicillin and 10 mg/ml streptomycin, Sigma). Cell cultures were performed at 37°C in a 5% CO₂/air atmosphere. Where indicated, cells were treated with vehicle or different concentrations of copper (Cu) for the indicated times.

siRNA knockdown of PrP^C and Transfection

The silencing PrP^C expression essay was performed following the protocol described in a previous report (32). The experiments where the expression of *PrP* gene was invalidated using siRNA strategy were performed in parallel of controlled experiments using scrambled siRNA. The presence of the transfectant reagent (*Lipofectamine*[®] 2000, France) and siRNA scramble did not affect the cell viability compared to the control (untreated) condition. The results are reported as supplementary data (Fig. S4-D).

Cells lysates

For the steady state expression and endoglycosidase experiments, cells were washed twice with ice-cold phosphate buffer saline (PBS) and lysed at 4°C for 20 min in PBS containing 1% NP40, 0.5% deoxycholic acid, and 0.1% SDS added with protease inhibitors (10 mM PMSF, 1 μM leupeptin/pepstatin A and 1mg/ml of iodoacetamide). For proteinase K (PK) treatment, cells were lysed in PBS containing 100 mM NaCl, 10 mM Tris, 10 mM EDTA, 0.5% NP-40, 0.5% deoxycholic acid, pH 7.4. Protein concentrations were measured using the Micro BCA protein assay kit (Thermo Scientific, France).

Endoglycosidase and proteinase K (PK) digestion

To distinguish between high mannose and complex-type N-linked oligosaccharide modification of PrP^C, cell lysates were incubated with endoglycosidase H (H) and peptide N-glycosidase F (F) as previously reported (2). The mobility shift of deglycosylated PrP^C was visualized by immunoblotting using an anti-PrP mAb (SAF32). For PK treatment, cells lysates were incubated with 20μg/ml PK for 3h at 37°C, and the reaction was stopped by adding PMSF (3mM).

Immunoprecipitation, electrophoresis and immunoblotting

For immunoprecipitation assay, cells were lysed at 4°C for 30 min in PBS lysis solution containing 20 mM Tris HCl pH 8, 137 mM NaCl, 10% glycerol and 1% Nonidet P-40 (NP-40). Protein extracts were incubated 2 h with 1 μg/ml of anti-PrP^C antibody (SAF32) at 4°C, and immunoprecipitated with protein G-coupled sepharose beads (Sigma) for 2 h hours at 4°C.

All protein samples were denatured for 5 min at 90°C in 2.5% SDS final concentration of Laemelli Sample Buffer (LBS), subjected to an SDS-PAGE (12%), transferred onto nitrocellulose membranes (Bio-Rad) and probed with corresponding primary antibodies. The following antibodies were used: mouse anti-E-cadherin (Ecad, Ozyme, France), anti-desmoglein (Deg, Covalab, France), anti-Ki-67 (DAKO, France), anti-Na⁺/K⁺-ATPase (Hybridoma Bank, University of Iowa, Iowa), and rabbit anti-ZO-1 (Fisher Sc., France), anti- γ -catenin (γ -cat, Abcam), anti-occludin (Occ, Sigma, France), anti-desmoplakin (Dep, Covalab, France). The antigen-antibody reaction was revealed using IgG antibody coupled to HRP (Covalab, France) and developed with ECL (Bio-Rad, France) using Fusion FX7 (Vilbert Lourmat).

Cell surface biotinylation

To determine the cell surface expression of PrP^C protein, HBE cells were selectively biotinylated as described previously (18). Biotinylated PrP^C protein was isolated by immunoprecipitation on Streptavidin-Sepharose (Sigma-Aldrich) and visualized by immunoblotting using anti-PrP mAb. The amount of biotinylated PrP^C relative to the control (time (t) = 0) was quantified by scanning the gel lanes followed by analysis with the Scion Image program (<http://www.scioncorp.com/pages>).

Immunofluorescence microscopy

The indirect immunofluorescence has been done as described previously (18).

RNA isolation, RT, and real-time qPCR analysis

Total mRNA was extracted from cells and 1 μ g of the mRNA was reverse transcribed under conditions recommended by the manufacturer (Agilent technologies). The PCR was performed using the mouse (forward: 5'GTGTACTACAGGAAAGTGGATC3'; backward: 5'ACGACTGCGTCAATATCACCAT3') and human (forward: 5'CAAGCCGAGTAAGCCAAAACC3'; backward: 5'CCCATCATACATTCGGCAGTG) 3' primers and GoTaq[®] qPCR Master Mix provided by Promega. The primers were designed to amplify a 131 pb fragment of the human *PrP* gene in HTR, A549 and HBE cells and a 69 pb fragment of the mouse *PrP* gene in the N2a cells.

Prion mRNA expression was quantified by real-time RT-qPCR using CFX96[™] Real-Time detection system (Biorad) as previously described (66).

Cell viability using MTT test

Cells were cultured in 96 wells plate upon confluency. Depending on experiment, 0-200 μM CuSO_4 was added for 0-24 hours and followed by 4 h incubation in phenol red free medium containing 10% of MTT ([4,5-dimethylthiazol-2-yl]-2,5-diphenyl tetrazolium bromide, Sigma). The MTT solution was replaced by MTT lysis solution (10% Triton X-100 and 0.1 N HCl in anhydrous isopropanol), and the resulting optical density (DO) was determined after measurement of the difference between 570 nm and 690 nm absorbance.

Trans-epithelial resistance (TER) assay

Cells were seeded at confluency (day 0) on collagen-coated polycarbonate filters (Transwell-COL, Costar). TER was measured from day 1 to day 8 of cell culture using a Volt-Ohm Meter (Millipore, France).

Paracellular Permeability measurement

The rate of inulin diffusion across the HBE cell layer was measured 48h after transfection with siRNA-PrP^C or scrambled (control). Fluorescein isothiocyanate (FITC)-labeled inulin (Sigma, France) was dissolved in HBE cells medium at 100 $\mu\text{g}/\text{ml}$ and was introduced to the apical side of the cells. After 24 h incubation at 37°C, the media on the apical and basolateral side of the cells were collected. The concentration of FITC-inulin in the collected medium was measured using a fluorescent plate reader (TECAN, France) with 475 nm excitation and 500–550 nm emission. The apparent permeability was calculated as previously reported (15).

Intracellular copper determination

To evaluate the intracellular copper concentration, control and PrP^C-knockdown HBE cells were collected and stored at RT. Samples were vacuum-dried and mineralized in 70% nitric acid before analysis with Inductively Coupled Plasma-Atomic Emission Spectrometry (ICP-AES) with a Varian, Vista MPX instrument. The copper content (μg) was reported relatively to the number of cells (10^6).

ROS Measurements

Normal and PrP^C siRNA knockdown HBE cells (10^6 cells/well) were seeded in a 24-well plate and cultured for 24 h. The cells were washed and changed to serum-free media and incubated with 50 μM of 5-(and 6)-chloromethyl-2',7'-dichlorodihydrofluorescein

diacetate acetyl ester (H₂DCFDA, Invitrogen, France) for 45 min. The conversion of H₂DCFDA to fluorescent DCF was measured using a plate reader Infinite M200 (TECAN, France).

Statistical analysis

Statistical comparisons were made using Student's t-test analysis. Calculations were performed using SigmaStat (Jandel Scientific Software, SanRafael, CA).

Acknowledgments

We thank the staff of the Department of Medicine, Respiratory Division, (Pr. C. Pison) at the Hospital of Grenoble (CHU) for allowing access to human lung tissues.

We acknowledge the following sources of funding: CNRS (LCBM-UMR 5249), INSERM (U1036), UJF, and CEA/DSV/BIG), and VLM (Vaincre la Mucoviscidose, France). AK, is a fellowship from AGIR program (University of Grenoble). SC and JC are fellowships from VLM (Vaincre la mucoviscidose, France)

Author Disclosure Statement

There is no conflict of interest.

References

1. Aguzzi A, Baumann F, Bremer J. The prion's elusive reason for being. *Annu Rev Neurosci* 31: 439-77, 2008.
2. Alfaidy N, Chauvet S, Donadio-Andrei S, Salomon A, Saoudi Y, Richaud P, Aude-Garcia C, Hoffmann P, Andrieux A, Moulis JM, Feige JJ, Benharouga M. Prion protein expression and functional importance in developmental angiogenesis: role in oxidative stress and copper homeostasis. *Antioxid Redox Signal* 18: 400-11, 2013.
3. Arkhipenko A, Syan S, Victoria GS, Lebreton S, Zurzolo C. PrPC Undergoes Basal to Apical Transcytosis in Polarized Epithelial MDCK Cells. *PLoS One* 11: e0157991, 2016.
4. Baker RD, Baker SS, LaRosa K. Polarized Caco-2 cells. Effect of reactive oxygen metabolites on enterocyte barrier function. *Dig Dis Sci* 40: 510-8, 1995.
5. Banan A, Fields JZ, Zhang Y, Keshavarzian A. iNOS upregulation mediates oxidant-induced disruption of F-actin and barrier of intestinal monolayers. *Am J Physiol Gastrointest Liver Physiol* 280: G1234-46, 2001.
6. Basler K, Oesch B, Scott M, Westaway D, Walchli M, Groth DF, McKinley MP, Prusiner SB, Weissmann C. Scrapie and cellular PrP isoforms are encoded by the same chromosomal gene. *Cell* 46: 417-28, 1986.
7. Besnier LS, Cardot P, Da Rocha B, Simon A, Loew D, Klein C, Riveau B, Lacasa M, Clair C, Rousset M, Thenet S. The cellular prion protein PrPc is a partner of the Wnt pathway in intestinal epithelial cells. *Mol Biol Cell* 26: 3313-28, 2015.
8. Brown DR, Qin K, Herms JW, Madlung A, Manson J, Strome R, Fraser PE, Kruck T, von Bohlen A, Schulz-Schaeffer W, Giese A, Westaway D, Kretschmar H. The cellular prion protein binds copper in vivo. *Nature* 390: 684-7, 1997.
9. Buschmann A, Kuczius T, Bodemer W, Groschup MH. Cellular prion proteins of mammalian species display an intrinsic partial proteinase K resistance. *Biochem Biophys Res Commun* 253: 693-702, 1998.
10. Cantin AM, Hartl D, Konstan MW, Chmiel JF. Inflammation in cystic fibrosis lung disease: Pathogenesis and therapy. *J Cyst Fibros* 14: 419-30, 2015.
11. Castle AR, Gill AC. Physiological Functions of the Cellular Prion Protein. *Front Mol Biosci* 4: 19, 2017.

12. Caughey B, Neary K, Buller R, Ernst D, Perry LL, Chesebro B, Race RE. Normal and scrapie-associated forms of prion protein differ in their sensitivities to phospholipase and proteases in intact neuroblastoma cells. *J Virol* 64: 1093-101, 1990.
13. Christensen HM, Harris DA. A deleted prion protein that is neurotoxic in vivo is localized normally in cultured cells. *J Neurochem* 108: 44-56, 2009.
14. Collinge J. Human prion diseases and bovine spongiform encephalopathy (BSE). *Human Molecular Genetics* 6: 1699-1705, 1997.
15. Coyne CB, Vanhook MK, Gambling TM, Carson JL, Boucher RC, Johnson LG. Regulation of airway tight junctions by proinflammatory cytokines. *Mol Biol Cell* 13: 3218-34, 2002.
16. Cozens AL, Yezzi MJ, Yamaya M, Steiger D, Wagner JA, Garber SS, Chin L, Simon EM, Cutting GR, Gardner P. A transformed human epithelial cell line that retains tight junctions post crisis. *In Vitro Cellular & Developmental Biology: Journal of the Tissue Culture Association* 28A: 735-744, 1992.
17. Das D, Luo X, Singh A, Gu Y, Ghosh S, Mukhopadhyay CK, Chen SG, Sy MS, Kong Q, Singh N. Paradoxical role of prion protein aggregates in redox-iron induced toxicity. *PLoS One* 5: e11420, 2010.
18. De Keukeleire B, Donadio S, Micoud J, Lechardeur D, Benharouga M. Human cellular prion protein hPrPC is sorted to the apical membrane of epithelial cells. *Biochemical and Biophysical Research Communications* 354: 949-954, 2007.
19. Ferruzza S, Scacchi M, Scarino ML, Sambuy Y. Iron and copper alter tight junction permeability in human intestinal Caco-2 cells by distinct mechanisms. *Toxicol In Vitro* 16: 399-404, 2002.
20. Ferruzza S, Scarino ML, Rotilio G, Ciriolo MR, Santaroni P, Muda AO, Sambuy Y. Copper treatment alters the permeability of tight junctions in cultured human intestinal Caco-2 cells. *Am J Physiol* 277: G1138-48, 1999.
21. Forbes B, Shah A, Martin GP, Lansley AB. The human bronchial epithelial cell line 16HBE14o-as a model system of the airways for studying drug transport. *International Journal of Pharmaceutics* 257: 161-167, 2003.

22. Geys J, Coenegrachts L, Vercammen J, Engelborghs Y, Nemmar A, Nemery B, Hoet PH. In vitro study of the pulmonary translocation of nanoparticles: a preliminary study. *Toxicol Lett* 160: 218-26, 2006.
23. Giard DJ, Aaronson SA, Todaro GJ, Arnstein P, Kersey JH, Dosik H, Parks WP. In vitro cultivation of human tumors: establishment of cell lines derived from a series of solid tumors. *J Natl Cancer Inst* 51: 1417-23, 1973.
24. Gomes MP, Millen TA, Ferreira PS, e Silva NL, Vieira TC, Almeida MS, Silva JL, Cordeiro Y. Prion protein complexed to N2a cellular RNAs through its N-terminal domain forms aggregates and is toxic to murine neuroblastoma cells. *J Biol Chem* 283: 19616-25, 2008.
25. Gonzalez-Mariscal L, Namorado MC, Martin D, Luna J, Alarcon L, Islas S, Valencia L, Muriel P, Ponce L, Reyes JL. Tight junction proteins ZO-1, ZO-2, and occludin along isolated renal tubules. *Kidney Int* 57: 2386-402, 2000.
26. Grumbach Y, Quynh NV, Chiron R, Urbach V. LXA4 stimulates ZO-1 expression and transepithelial electrical resistance in human airway epithelial (16HBE14o-) cells. *Am J Physiol Lung Cell Mol Physiol* 296: L101-8, 2009.
27. Gu Y, Hinnerwisch J, Fredricks R, Kalepu S, Mishra RS, Singh N. Identification of cryptic nuclear localization signals in the prion protein. *Neurobiol Dis* 12: 133-49, 2003.
28. Haeberle AM, Ribaut-Barassin C, Bombarde G, Mariani J, Hunsmann G, Grassi J, Bailly Y. Synaptic prion protein immuno-reactivity in the rodent cerebellum. *Microsc Res Tech* 50: 66-75, 2000.
29. Haldar S, Tripathi A, Qian J, Beserra A, Suda S, McElwee M, Turner J, Hopfer U, Singh N. Prion protein promotes kidney iron uptake via its ferrireductase activity. *J Biol Chem* 290: 5512-22, 2015.
30. Harris DA. Cellular biology of prion diseases. *Clin Microbiol Rev* 12: 429-44, 1999.
31. Hiemstra PS, McCray PB, Jr., Bals R. The innate immune function of airway epithelial cells in inflammatory lung disease. *Eur Respir J* 45: 1150-62, 2015.
32. Hoffmann P, Saoudi Y, Benharouga M, Graham CH, Schaal J-P, Mazouni C, Feige J-J, Alfaidy N. Role of EG-VEGF in human placentation: Physiological and pathological implications. *Journal of Cellular and Molecular Medicine* 13: 2224-2235, 2009.

33. Hu W, Kieseier B, Frohman E, Eagar TN, Rosenberg RN, Hartung HP, Stuve O. Prion proteins: physiological functions and role in neurological disorders. *J Neurol Sci* 264: 1-8, 2008.
34. Ikenouchi J, Sasaki H, Tsukita S, Furuse M, Tsukita S. Loss of occludin affects tricellular localization of tricellulin. *Mol Biol Cell* 19: 4687-93, 2008.
35. Jackson GS, Murray I, Hosszu LL, Gibbs N, Waltho JP, Clarke AR, Collinge J. Location and properties of metal-binding sites on the human prion protein. *Proc Natl Acad Sci U S A* 98: 8531-5, 2001.
36. John LJ, Fromm M, Schulzke JD. Epithelial barriers in intestinal inflammation. *Antioxid Redox Signal* 15: 1255-70, 2011.
37. Johnson LN, Koval M. Cross-talk between pulmonary injury, oxidant stress, and gap junctional communication. *Antioxid Redox Signal* 11: 355-67, 2009.
38. Khosravani H, Zhang Y, Tsutsui S, Hameed S, Altier C, Hamid J, Chen L, Villemaire M, Ali Z, Jirik FR, Zamponi GW. Prion protein attenuates excitotoxicity by inhibiting NMDA receptors. *J Cell Biol* 181: 551-65, 2008.
39. Kohler K, Louvard D, Zahraoui A. Rab13 regulates PKA signaling during tight junction assembly. *J Cell Biol* 165: 175-80, 2004.
40. Linsenmeier L, Altmeyen HC, Wetzel S, Mohammadi B, Saftig P, Glatzel M. Diverse functions of the prion protein - Does proteolytic processing hold the key? *Biochim Biophys Acta* 1864: 2128-2137, 2017.
41. Llorens F, Ansoleaga B, Garcia-Esparcia P, Zafar S, Grau-Rivera O, Lopez-Gonzalez I, Blanco R, Carmona M, Yague J, Nos C, Del Rio JA, Gelpi E, Zerr I, Ferrer I. PrP mRNA and protein expression in brain and PrP(c) in CSF in Creutzfeldt-Jakob disease MM1 and VV2. *Prion* 7: 383-93, 2013.
42. MacNee W, Rahman I. Oxidants/antioxidants in idiopathic pulmonary fibrosis. *Thorax* 50 Suppl 1: S53-8, 1995.
43. McKinley MP, Taraboulos A, Kenaga L, Serban D, Stieber A, DeArmond SJ, Prusiner SB, Gonatas N. Ultrastructural localization of scrapie prion proteins in cytoplasmic vesicles of infected cultured cells. *Lab Invest* 65: 622-30, 1991.

44. Mishra RS, Basu S, Gu Y, Luo X, Zou W-Q, Mishra R, Li R, Chen SG, Gambetti P, Fujioka H, Singh N. Protease-resistant human prion protein and ferritin are cotransported across Caco-2 epithelial cells: implications for species barrier in prion uptake from the intestine. *The Journal of Neuroscience: The Official Journal of the Society for Neuroscience* 24: 11280-11290, 2004.
45. Mittal M, Thiruvengkatachari B, Sandler PJ, Benson PE. A three-dimensional comparison of torque achieved with a preadjusted edgewise appliance using a Roth or MBT prescription. *Angle Orthod* 85: 292-7, 2015.
46. Miura T, Hori-i A, Mototani H, Takeuchi H. Raman spectroscopic study on the copper(II) binding mode of prion octapeptide and its pH dependence. *Biochemistry* 38: 11560-9, 1999.
47. Mo GW, Cai SX, Zhao HJ, Li WJ, Tong WC, Liu LY. [Effect of toluene diisocyanate on reactive oxygen species production and permeability of human bronchial epithelial cells in vitro]. *Nan Fang Yi Ke Da Xue Xue Bao* 31: 239-43, 2011.
48. Monnet C, Marthiens V, Enslin H, Frobert Y, Sobel A, Mege RM. Heterogeneity and regulation of cellular prion protein glycoforms in neuronal cell lines. *Eur J Neurosci* 18: 542-8, 2003.
49. Morel E, Fouquet S, Chateau D, Yvernault L, Frobert Y, Pinçon-Raymond M, Chambaz J, Pillot T, Rousset M. The cellular prion protein PrPc is expressed in human enterocytes in cell-cell junctional domains. *The Journal of Biological Chemistry* 279: 1499-1505, 2004.
50. Morel E, Fouquet S, Strup-Perrot C, Thievend CP, Petit C, Loew D, Faussat A-M, Yvernault L, Pinçon-Raymond M, Chambaz J, Rousset M, Thenet S, Clair C. The Cellular Prion Protein PrPc Is Involved in the Proliferation of Epithelial Cells and in the Distribution of Junction-Associated Proteins. *PLoS ONE* 3: e3000, 2008.
51. Nawijn MC, Hackett TL, Postma DS, van Oosterhout AJ, Heijink IH. E-cadherin: gatekeeper of airway mucosa and allergic sensitization. *Trends Immunol* 32: 248-55, 2011.
52. Paquet S, Sabuncu E, Delaunay J-L, Laude H, Vilette D. Prion Infection of Epithelial Rov Cells Is a Polarized Event. *Journal of Virology* 78: 7148-7152, 2004.
53. Pauly PC, Harris DA. Copper stimulates endocytosis of the prion protein. *J Biol Chem* 273: 33107-10, 1998.

54. Petit CS, Besnier L, Morel E, Rousset M, Thenet S. Roles of the cellular prion protein in the regulation of cell-cell junctions and barrier function. *Tissue Barriers* 1: e24377, 2013.
55. Pfeifer K, Bachmann M, Schroder HC, Forrest J, Muller WE. Kinetics of expression of prion protein in uninfected and scrapie-infected N2a mouse neuroblastoma cells. *Cell Biochem Funct* 11: 1-11, 1993.
56. Provansal M, Roche S, Pastore M, Casanova D, Belondrade M, Alais S, Leblanc P, Windl O, Lehmann S. Proteomic consequences of expression and pathological conversion of the prion protein in inducible neuroblastoma N2a cells. *Prion* 4: 292-301, 2010.
57. Prusiner SB. Molecular biology of prion diseases. *Science* 252: 1515-22, 1991.
58. Puchelle E, Zahm JM, Tournier JM, Coraux C. Airway epithelial repair, regeneration, and remodeling after injury in chronic obstructive pulmonary disease. *Proc Am Thorac Soc* 3: 726-33, 2006.
59. Puig B, Altmepfen HC, Thurm D, Geissen M, Conrad C, Braulke T, Glatzel M. N-glycans and glycosylphosphatidylinositol-anchor act on polarized sorting of mouse PrP(C) in Madin-Darby canine kidney cells. *PLoS One* 6: e24624, 2011.
60. Rachidi W, Vilette D, Guiraud P, Arlotto M, Riondel J, Laude H, Lehmann S, Favier A. Expression of prion protein increases cellular copper binding and antioxidant enzyme activities but not copper delivery. *J Biol Chem* 278: 9064-72, 2003.
61. Rao RK, Baker RD, Baker SS, Gupta A, Holycross M. Oxidant-induced disruption of intestinal epithelial barrier function: role of protein tyrosine phosphorylation. *Am J Physiol* 273: G812-23, 1997.
62. Sarnataro D, Paladino S, Campana V, Grassi J, Nitsch L, Zurzolo C. PrPC is sorted to the basolateral membrane of epithelial cells independently of its association with rafts. *Traffic* 3: 810-21, 2002.
63. Sauer H, Wefer K, Vetrugno V, Pocchiari M, Gissel C, Sachinidis A, Hescheler J, Wartenberg M. Regulation of intrinsic prion protein by growth factors and TNF-alpha: the role of intracellular reactive oxygen species. *Free Radic Biol Med* 35: 586-94, 2003.
64. Stahl N, Borchelt DR, Prusiner SB. Differential release of cellular and scrapie prion proteins from cellular membranes by phosphatidylinositol-specific phospholipase C. *Biochemistry* 29: 5405-12, 1990.

65. Sussan TE, Gajghate S, Chatterjee S, Mandke P, McCormick S, Sudini K, Kumar S, Breyse PN, Diette GB, Sidhaye VK, Biswal S. Nrf2 reduces allergic asthma in mice through enhanced airway epithelial cytoprotective function. *Am J Physiol Lung Cell Mol Physiol* 309: L27-36, 2015.
66. Traboulsi W, Sergent F, Boufettal H, Brouillet S, Slim R, Hoffmann P, Benlahfid M, Zhou QY, Balboni G, Onnis V, Bolze PA, Salomon A, Sauthier P, Mallet F, Aboussaouira T, Feige JJ, Benharouga M, Alfaidy N. Antagonism of EG-VEGF Receptors as Targeted Therapy for Choriocarcinoma Progression In Vitro and In Vivo. *Clin Cancer Res* 23: 7130-7140, 2017.
67. Uelhoff A, Tatzelt J, Aguzzi A, Winklhofer KF, Haass C. A pathogenic PrP mutation and doppel interfere with polarized sorting of the prion protein. *J Biol Chem* 280: 5137-40, 2005.
68. Villegas L, Stidham T, Nozik-Grayck E. Oxidative Stress and Therapeutic Development in Lung Diseases. *J Pulm Respir Med* 4, 2014.
69. Vivekananda J, Lin A, Coalson JJ, King RJ. Acute inflammatory injury in the lung precipitated by oxidant stress induces fibroblasts to synthesize and release transforming growth factor- α . *J Biol Chem* 269: 25057-61, 1994.
70. Waggoner DJ, Drisaldi B, Bartnikas TB, Casareno RL, Prohaska JR, Gitlin JD, Harris DA. Brain copper content and cuproenzyme activity do not vary with prion protein expression level. *J Biol Chem* 275: 7455-8, 2000.
71. Watt NT, Taylor DR, Gillott A, Thomas DA, Perera WS, Hooper NM. Reactive oxygen species-mediated beta-cleavage of the prion protein in the cellular response to oxidative stress. *J Biol Chem* 280: 35914-21, 2005.
72. Winterbourn CC. Toxicity of iron and hydrogen peroxide: the Fenton reaction. *Toxicol Lett* 82-83: 969-74, 1995.
73. Zeng F, Watt NT, Walmsley AR, Hooper NM. Tethering the N-terminus of the prion protein compromises the cellular response to oxidative stress. *J Neurochem* 84: 480-90, 2003.

List of Abbreviations

Cu: Copper

DCF: dichlorofluorescein

16HBE14o- (HBE): Human Bronchial Epithelial cells

GPI: Glycosyl Phosphatidyl Inositol

CF: Cystic fibrosis

PrP^C: Cellular Prion Protein

ROS: Reactive Oxygen Species

Figure legends

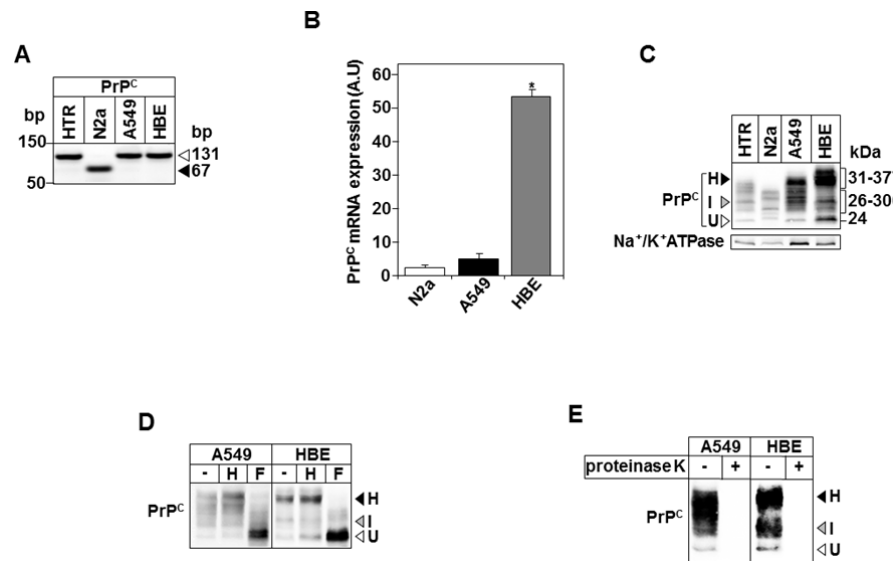


Figure 1: Steady state expression and characterization of PrP^C protein in human bronchial epithelial cells (HBE). **(A)** RT-qPCR of PrP^C mRNA in HTR, N2a, A549 and HBE cells. **(B)** The expression levels of PrP^C mRNAs were quantified by real-time RT-qPCR, normalized to the 18S levels. Data are expressed as mean ± SE (n=4). **(C)** Immunoblot detection of PrP^C in protein extracts from N2a, HTR, A549 and HBE cells. **(D)** Endoglycosidase H (H) and N-glycosidase F (F) digestion profiles of PrP^C protein. **(E)** PrP^C digestion with 20 µg/ml of proteinase K (PK) for 1 hour at 37°C. **(C, D, E)** Equal amounts of protein extracts from the indicated cell lines were separated on 12% SDS-PAGE, transferred to nitrocellulose, and immunoblotted using the monoclonal anti-PrP antibody (SAF-32). The high- (H), intermediate- (I), and unglycosylated (U) forms are indicated, respectively, by black, gray, and white arrowheads.

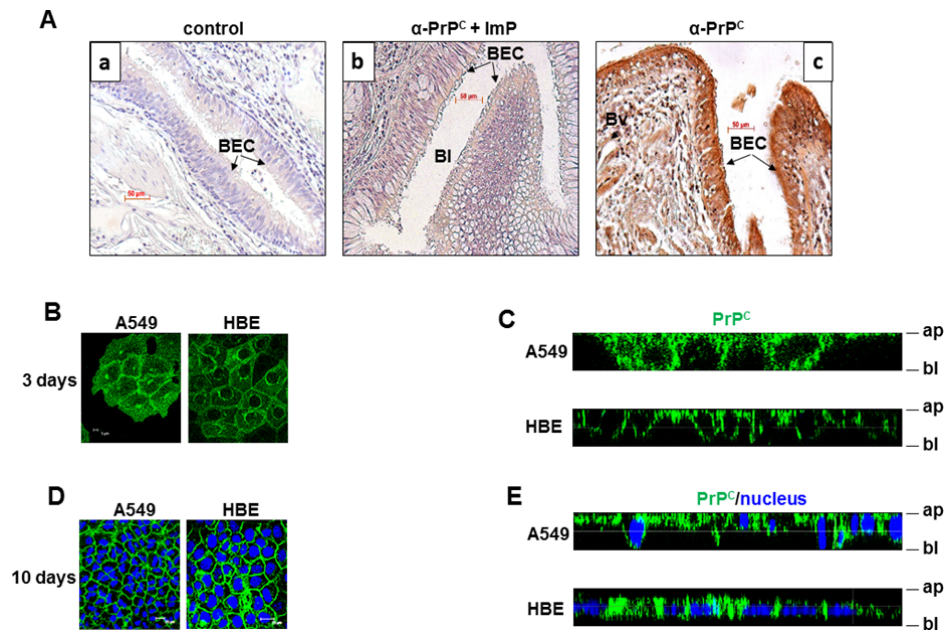


Figure 2: Localization of PrP^C protein in human bronchial epithelial tissue and cells. **(A)** Immunolocalization of PrP^C using mAb anti-PrP (SAF-32) in human bronchial tissue (c). (a) and (b) correspond to the negative controls using the secondary antibody alone (a) or the SAF-32 mAb preincubated (ImP) for 24h at 4°C with the corresponding antigenic peptide (b). Asterisks in panels (b) show the strongest sites of PrP^C immunoreactivity. Bl, bronchial lumen, BEC, bronchial epithelial cells. **(B-E)** Immunofluorescence labeling of PrP^C (green, MAb anti-PrP) and nuclei (bleu, Hoechst) was performed after 3 or 10 days of HBE culture, **(C and E)** X/Z projections were reconstructed from horizontal optical sections of labeled cells at 3 and 10 days of confluency. ap, apical, bl, basolateral (n=4).

“To see this illustration in color, the reader is referred to the online version of this article at www.liebertpub.com/ars”

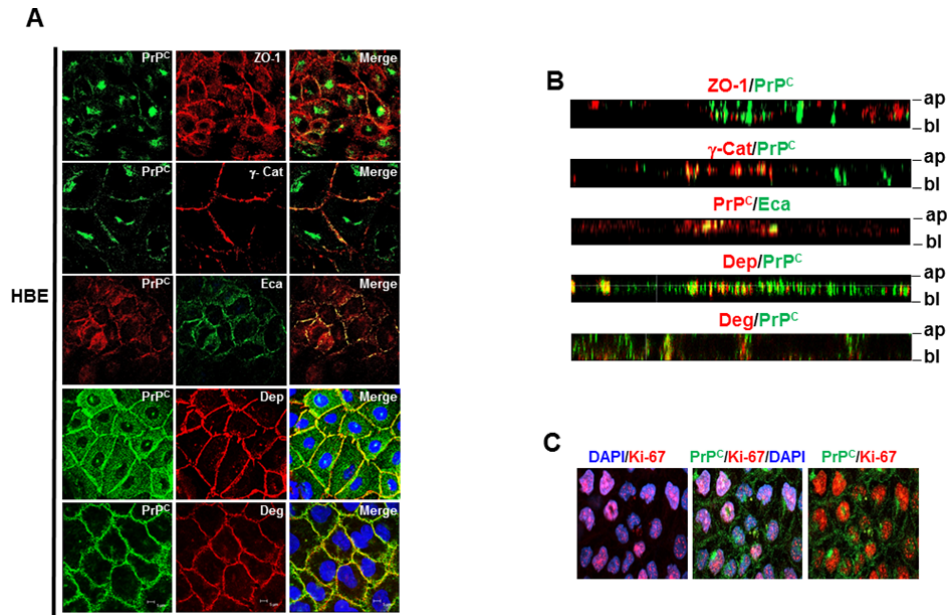


Figure 3: Colocalization of PrP^C protein with different proteins of the junctional barrier in polarized HBE cells. **(A)** Co-immunofluorescence labeling of PrP^C, zona occludens-1 (ZO-1), γ -catenin (γ -Cat), E-cadherin (Eca), desmoplakin (Dep), desmoglein (Des) and nuclei (blue, Hoechst) was performed in polarized HBE cells at day 10 of culture. **(B)** X/Z projections were reconstructed from horizontal optical section of labeled HBE cells at 10 days confluency. ap, apical, bl, basolateral. **(C)** Co-immunofluorescence labeling of PrP^C, Ki-67 protein and nuclei (blue, Hoechst) was performed in polarized HBE cells at day 10 of culture (n=4).

"To see this illustration in color, the reader is referred to the online version of this article at www.liebertpub.com/ars"

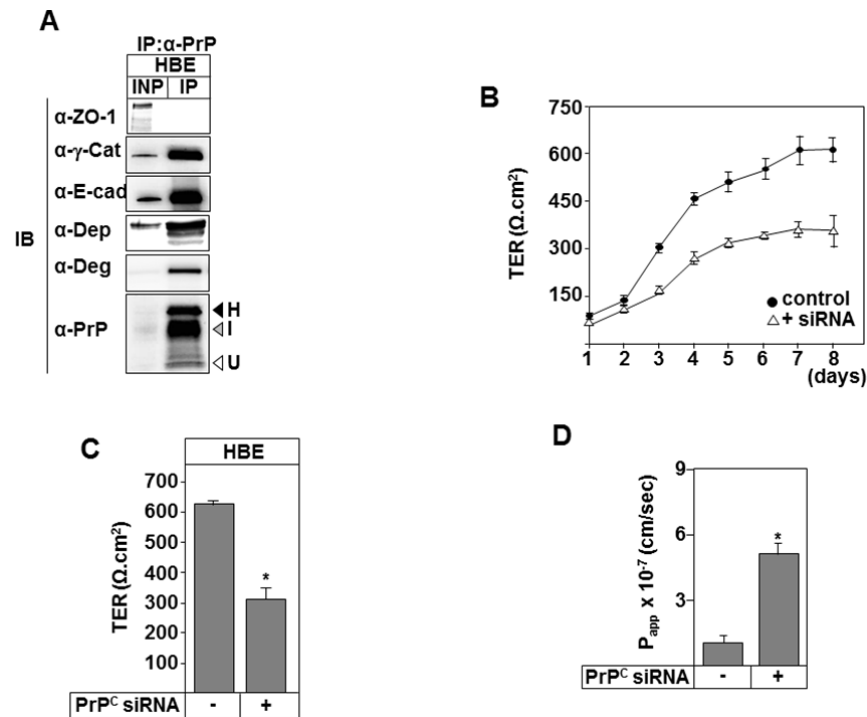


Figure 4: Interaction profiles and role of PrP^C protein in bronchial epithelial barrier. **(A)** PrP^C was immunoprecipitated (IP) using anti-PrP mAb (SAF32) and protein G coupled to sepharose. The eluted proteins were subjected to immunoblots (IB) using anti-PrP, anti-ZO-1, anti-γ-Cat (γ-Catenin) anti-Ecad (E-cadherin), anti-desmoplakin (Dsp) or anti-desmoglein (Deg). IN: input (10% of the protein extract before immunoprecipitation). The high- (H), intermediate- (I), and unglycosylated (U) forms are indicated, respectively, by black, gray, and white arrowheads. **(B)** Trans-epithelial resistance (TER) measurement in control (si-Scramble ●) and PrP^C-knockdown HBE cells (Δ). Cells were seeded at confluency (day 0) on collagen-coated polycarbonate filters and TER was assessed daily for 8 days. **(C)** TER values measured after 8 days of culture were plotted for the control (-) and PrP^C-knockdown (+) HBE cells. Values overwritten with stars are significantly different from the control ($p < 0.05$, $n=4$). **(D)** Paracellular permeability of HBE cells. FITC labeled-inulin was added to the apical chamber of si-Scramble (-) or PrP^C-knockdown HBE cells. Following 24h incubation at 37°C, the basolateral medium was removed for fluorescence measurement, and P_{app} (permeability apparent) was calculated. Results represent the mean of four independent experiments carried out in triplicate; bars represent the mean \pm SE ($P < 0.05$).

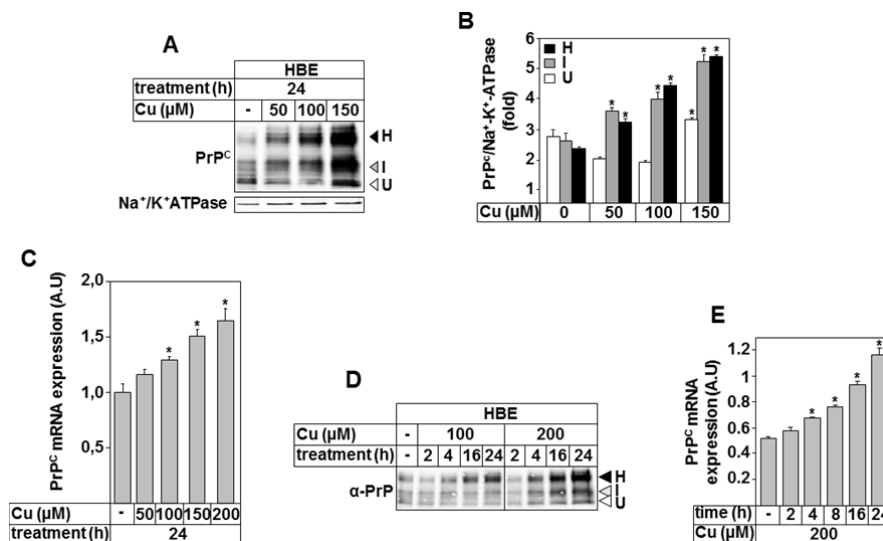


Figure 5: Copper treatment increases PrP^C expression in HBE cells. **(A, D)** HBE cells were treated with copper sulfate in a dose (μM) and time (h) dependent manner and cell lysates were subjected to immunoblots using anti-PrP (SAF-32) or anti-Na⁺/K⁺-ATPase antibody. The high- (H), intermediate- (I), and unglycosylated (U) forms are indicated, respectively, by black, white, and gray arrowheads. **(B)** ImageJ quantification of the expression of the three glycosylation forms of PrP^C protein standardized to Na⁺/K⁺-ATPase expression in HBE cells. **(C, E)** Following copper treatment, PrP^C mRNAs expression levels were quantified by real-time RT-PCR, normalized to the 18S levels and plotted as function of incubation time (h) and concentration (μM). A.U: arbitrary unit. Data are expressed as mean ± SE (n=6). Values overwritten with stars are significantly different from the control (0 h) (P < 0.05).

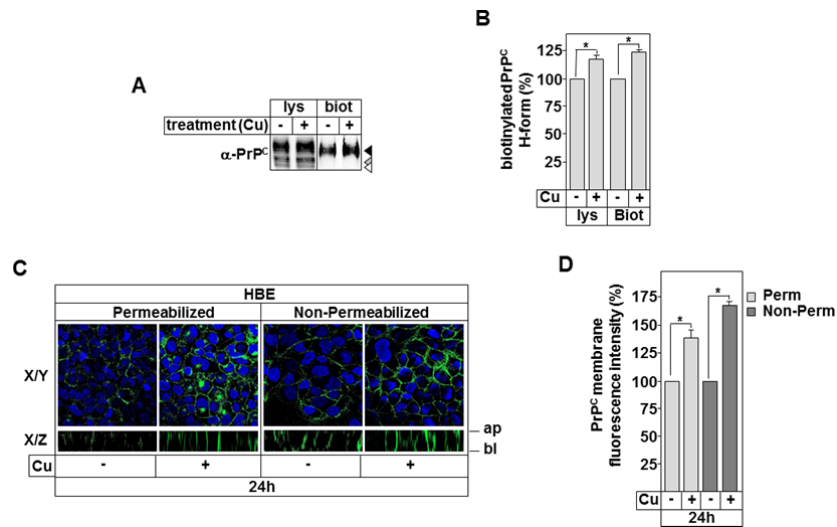


Figure 6: Copper treatment stimulates lateral membrane insertion of PrP^C protein.

(A) Detection of biotinylated PrP^C protein in HBE cells extract before (lysate, lys) and after biotinylation (biot) was achieved after 24h stimulation (+) of HBE cells with 100 μM of copper. PrP^C was covalently labelled with NHS-SS-biotin at 4°C. Biotinylated (biot) PrP^C was affinity-isolated on streptavidin (strep) beads and immunoblotted with anti-PrP mAb (SAF32). Neither intermediate- (I, white arrowheads) nor unglycosylated (U, gray arrowheads) forms were susceptible to biotinylation. (B) Biotinylated high-glycosylated form of PrP^C quantified using Image J was plotted as function of copper stimulation. Data are expressed as mean ± SE (n=3). Values with asterisk are significantly different from the control (0 h) (P < 0.05). (C) Immunofluorescence detection of PrP^C (green, MAb anti-PrP) in polarized HBE cells (10 days of culture) was performed following 24 h copper stimulation under non- and permeabilized conditions. ap, apical, bl, basolateral. X/Y and X/Z projections were reconstructed from horizontal optical sections. After 10 days of culture, nuclei were stained using Hoechst. (D) Lateral fluorescence labeling of HBE X/Z projection detected after 24 h copper treatment in non- and in permeabilized HBE cells (X/Z projection) was quantified using Image J and plotted as function of copper stimulation. Data are expressed as mean ± SE (n=3). Values with asterisk are significantly different from the control (-) (P < 0.05).

“To see this illustration in color, the reader is referred to the online version of this article at www.liebertpub.com/ars”

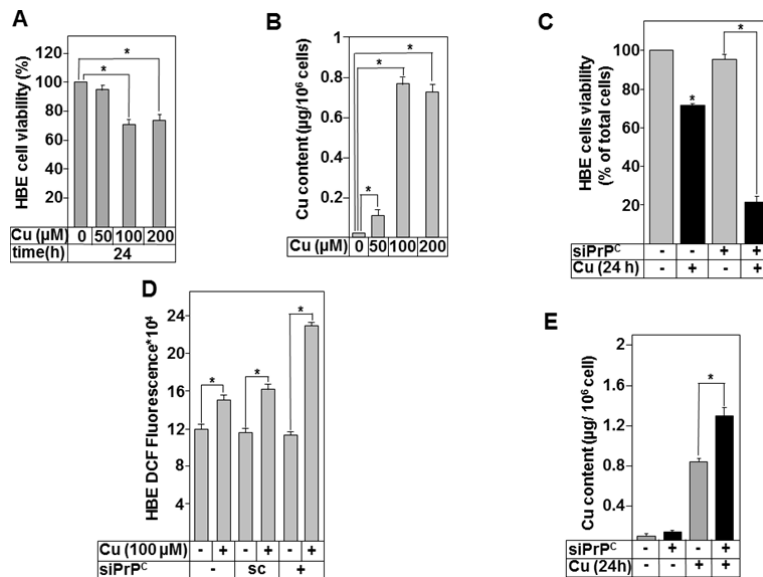


Figure 7: Depletion of PrP^C in HBE cells enhances Cu-induced pro-oxidants accumulation, increases cell Cu content and causes acute cell death. (**A**, **C**) Control (si-Scramble) or PrP-knockdown HBE cells (siPrP^C) were incubated in the absence or the presence of Cu for the indicated times. Cells were trypsinized and harvested. Dead cells were assessed by trypan blue staining and MTT assays. For Fig. 7C, 100 μM of Cu was used. (**B**, **E**) ICP-AES determination of Cu content in HBE cells under basal and following 24 h stimulation with Cu of wt and PrP^C depleted HBE cells (siPrP^C). For Fig. 7E, 100 μM of copper was used. (**D**) HBE or PrP-knockdown HBE cells (siPrP^C) were incubated with 50 μM DCFH-DA for 45 min. Cells were then incubated with or without 100 μM of Cu at 37°C for 2 h. DCF fluorescence was determined at an excitation wavelength of 485 nm and emission wavelength of 538 nm by a microplate reader. Data are expressed as mean \pm SE (n=6). Values with an asterisk are significantly different from the corresponding control ($P < 0.05$).

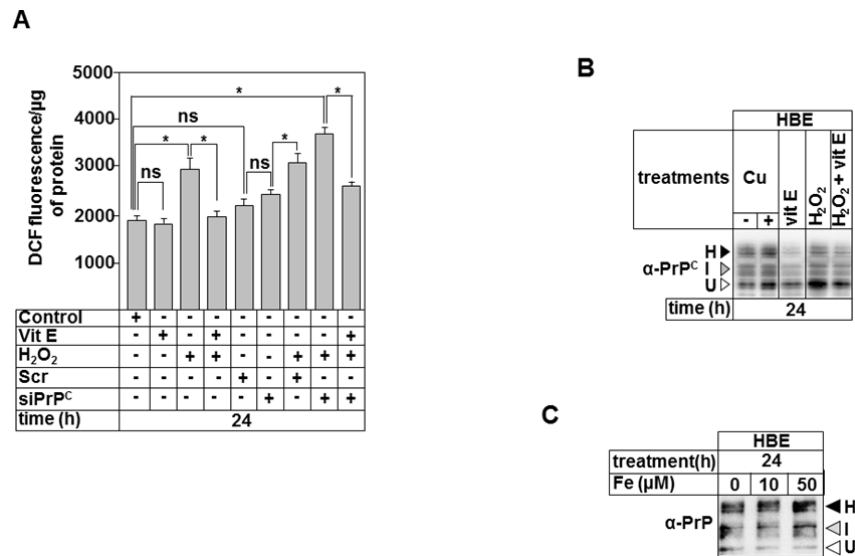


Figure 8: PrP^C protein responds to other pro-oxidants stimuli. **(A)** Control, si-Scramble (Scr), or PrP-knockdown HBE cells (siPrP^C) were cultured for 24h in the absence or in the presence of 100 μM of Trolox (vitamin E; Vit E), 100 μM of H₂O₂, or in the presence of both molecules. Oxidative stress evaluation was achieved by incubating the cells with 50 μM of DCFH-DA for 45 min. DCF fluorescence was determined at an excitation wavelength of 485 nm and emission wavelength of 538 nm by a microplate reader. Data are expressed as mean ± SE (n=4). Values with an asterisk are significantly different from the corresponding control (P < 0.05). **(B)** Detection of PrP^C protein in HBE cells extract following 24h treatment with 50 μM of copper (Cu), 100 μM of Vit E, 100 μM of H₂O₂ or a combination of Vit E and H₂O₂. PrP^C was immunoblotted with anti-PrP mAb (SAF-32). **(C)** HBE cells were treated with iron sulfate in a dose (μM) dependent manner and cell lysates were subjected to immunoblots using anti-PrP (SAF-32) or anti-Na⁺/K⁺-ATPase antibody. The high- (H), intermediate- (I), and unglycosylated (U) forms are indicated, respectively, by black, white, and gray arrowheads.

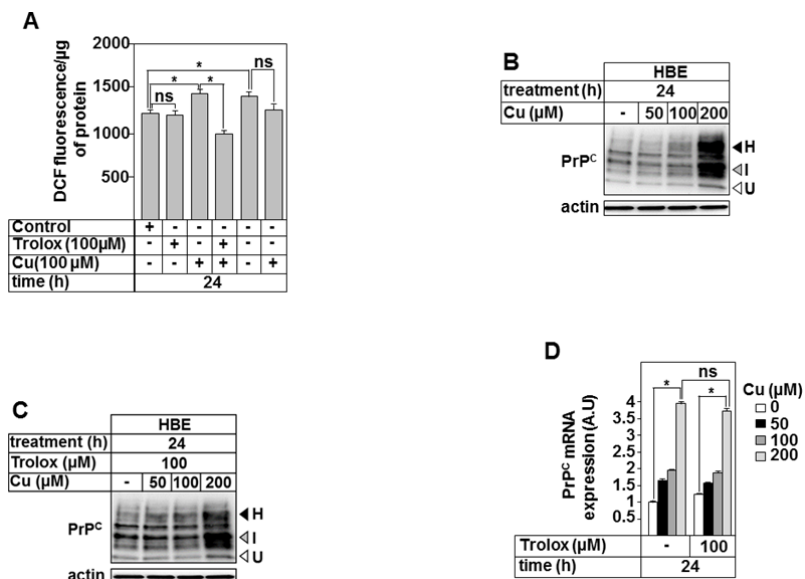


Figure 9: Copper increases PrP^C protein expression via a transcriptional pathway.

(A) HBE cells were cultured for 24h in the absence or in the presence of 100 μM of Trolox (vitamin E; Vit E), 100 μM of Cu, or in the presence of both molecules. Oxidative stress evaluation was achieved as described in figure 8A. Data are expressed as mean ± SE (n=4). Values with an asterisk are significantly different from their corresponding controls (P < 0.05). (B and C) report the detection of PrP^C protein in HBE cells extracts following 24h treatment with different concentrations of copper; Cu alone (B) or in combination with 100 μM of Trolox (C). (D) reports PrP^C mRNAs expression levels following 24h treatment with different concentrations of copper (Cu) alone or with 100 μM of Trolox. PrP^C mRNAs expression were quantified by real-time RT-PCR, normalized to the 18S levels and plotted as function of concentration of copper (μM). A.U: arbitrary unit. Data are expressed as mean ± SE (n=6). Values overwritten with stars are significantly different from the control (0 h) (P < 0.05).

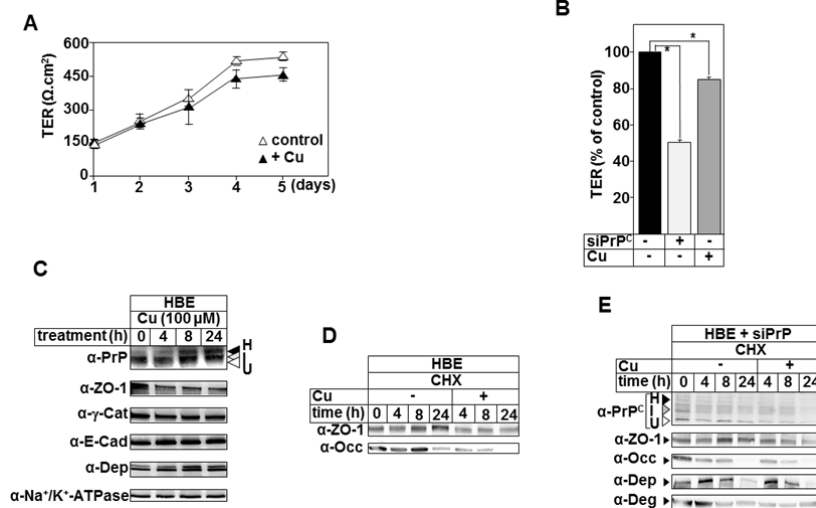


Figure 10: PrP^C protects adherent and desmosome proteins from oxidative-associated degradation.

(A) Trans-epithelial resistance (TER) measurement in control (Δ) and in the presence of 100 μM of copper (▲) for the indicated time. Cells were seeded at confluency (day 0) on collagen-coated polycarbonate filters and TER was assessed daily for 5 days. (B) TER values measured after 4 days of culture were plotted for the control (si-Scramble) and PrP^C-knockdown (+) HBE cells. Values overwritten with stars are significantly different from the control ($p < 0.05$).

(C) Steady state expression of tight (ZO-1 and occludin (Occ)), adherent (γ-catenin (γ-Cat) and E-cadherin (E-Cad)) and desmosome (desmoplakin (Dep)) junctional proteins following 100 μM copper treatment for the indicated times. Proteins were detected using the indicated antibodies. Anti-Na⁺/K⁺-ATPase was used as a loading control. The high- (H), intermediate- (I), and unglycosylated (U) forms of PrP^C protein are indicated, respectively, by black, gray, and white arrowheads.

(D) Degradation rate of ZO-1 and occludin (Occ) using cycloheximide (CHX) assays. For the indicated times, HBE cells were incubated in the presence of 100 μg/ml of CHX and in the absence (-) or presence (+) of 100 μM of copper. Protein extracts were separated on SDS-PAGE gels and proteins of interest were detected using anti-ZO-1 and anti-occludin antibodies.

(E) Degradation rate of PrP^C, ZO-1, occludin (Occ), desmoplakin (Dep) and desmoglein (Deg) in PrP^C-knockdown HBE cells (si-PrP) using cycloheximide (CHX) assays. For the

indicated times, si-PrP HBE cells were incubated in the presence of 100 $\mu\text{g}/\text{ml}$ of CHX and in the absence (-) or presence (+) of 100 μM of copper. Proteins extract were separated on SDS-PAGE gels and proteins of interest were detected using anti-ZO-1, anti-occludin, and-desmoplakin and anti-desmoglein antibodies.

Figures Legends of Supplementary figures

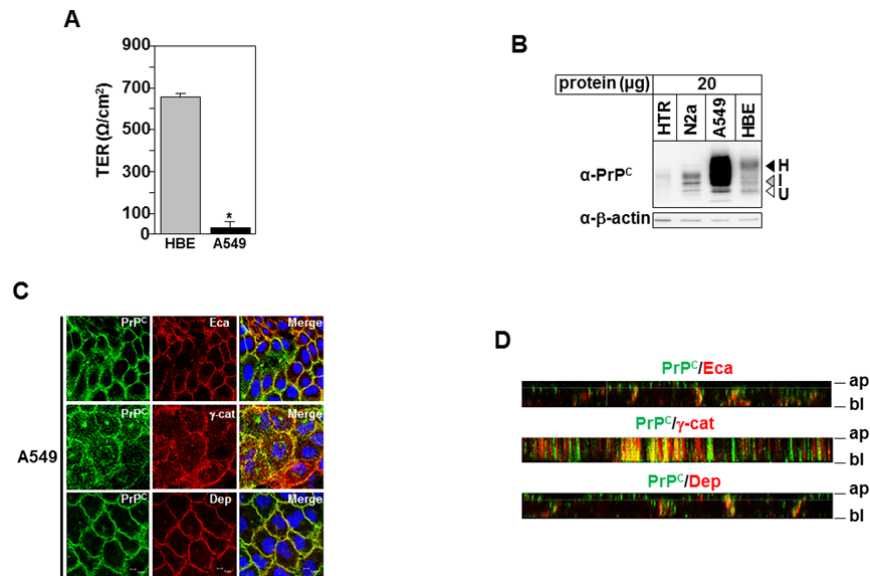


Figure S1: Trans-epithelial resistance (TER), expression, and localization of PrP^C and junctional proteins in A549 cells.

(A) TER measurement in HBE and A549 cells. HBE and A549 cells were seeded at a density of 20,000 cells/cm² on HTS 24-Transwell® filter plates. The changes in the TER were measured every day for 10 days, and the reported results corresponded to the values obtained at days 10. Each data point represents the mean ± SD (n=12 for A549 and HBE).

(B) Immunoblot detection of PrP^C protein in HTR, N2a, A549 and HBE cells. Equal amounts of protein extracts (20 μg) from the indicated cell lines were separated on 12% SDS-PAGE, transferred into nitrocellulose, and immunoblotted using the monoclonal anti-PrP antibody (SAF-32). The high- (H), intermediate- (I), and unglycosylated (U) forms are indicated, respectively by black, gray, and white arrowheads. β-actin (40 kDa) was detected as an internal loading control. **(C)** PrP^C colocalization with E-cadherin (E-cad), γ-catenin (γ-Cat) and desmoplakin (Dep) in A549 cells. **(D)** X/Z projections were reconstructed from horizontal optical section of labelled A549 cells at 10 days confluency.

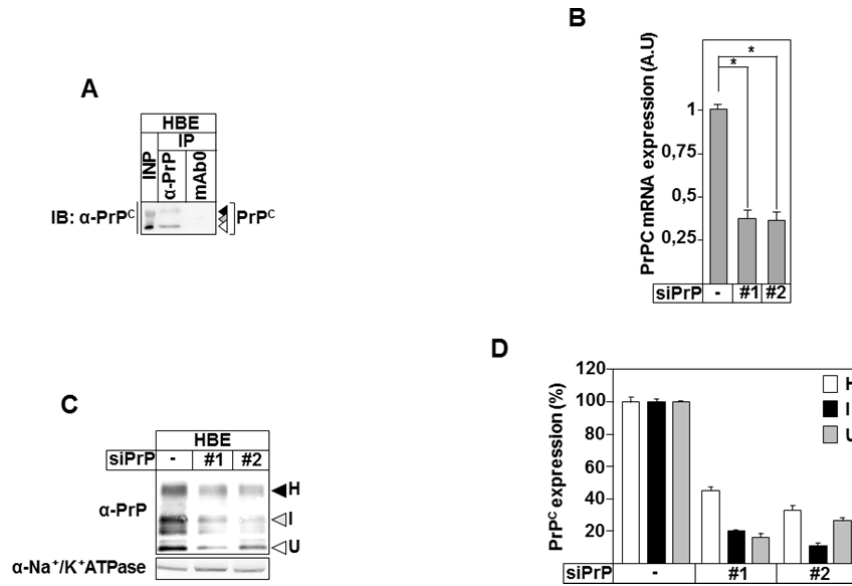


Figure S2: PrP^C immunoprecipitation control and PrP^C knockdown in HBE cells.

(B-C) PrP^C knockdown using two specific siRNA (#1 and #2). 48 h after transfection. mRNA and proteins were isolated and quantified by RT-qPCR (B) and by western blot using SAF-32 mAb (C) and image J analysis (D). Data are expressed as mean ± SE (n=4). Values overwritten with stars are significantly different from the control (0 h) (P < 0.05).

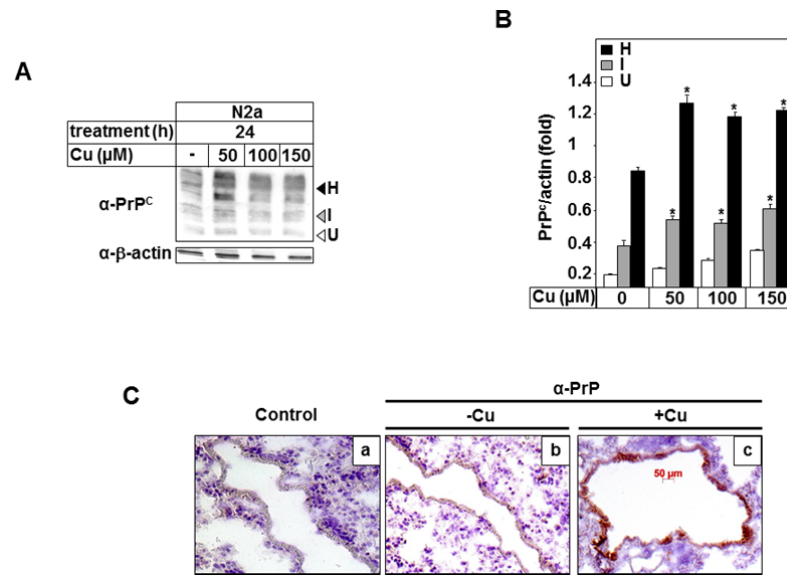
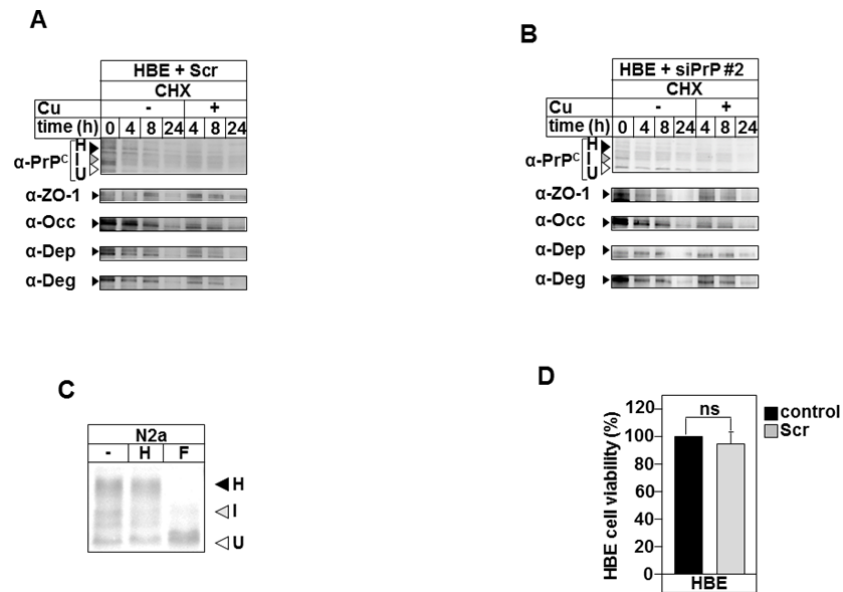


Figure S3: Copper stimulation increased PrP^C protein expression in mice bronchial epithelial tissue and in N2a neuroblastoma cells.

(A) Immunolocalization of PrP^C using mAb anti-PrP (SAF32) in mice bronchial tissue in the absence (b) or in the presence of copper treatment (c). (a) Negative controls.

(B) N2a cells were treated with copper sulfate in a dose (μM) dependent manner and cell lysates were subjected to immunoblots using anti-PrP (SAF-32) or anti- β -actin antibody. The high- (H), intermediate- (I), and unglycosylated (U) forms are indicated, respectively, by black, white, and gray arrowheads. **(C)** ImageJ quantification of the expression of the three glycosylation forms of PrP^C protein standardized to Na⁺/K⁺-ATPase expression in HBE cells. Data are expressed as mean \pm SE (n=4). Values overwritten with stars are significantly different from the control (0 h) (P < 0.05).

**Figure S4:**

(A-B) Degradation rate of PrP^C, ZO-1, occludin (Occ), desmoplakin (Dep), and desmoglein (Deg) in si-Scramble (Scr) (A) or PrP^C-knockdown or HBE cells (si-PrP (43)) (B) using cycloheximide (CHX) assays. For the indicated times, si-PrP HBE cells were incubated in the presence of 100 µg/ml of CHX and in the absence (-) or presence (+) of 100 µM of copper. Proteins extract were separated on SDS-PAGE gels and proteins of interest were detected using anti-ZO-1, anti-occludin, anti-desmoplakin and anti-desmoglein antibodies.

(C) Endoglycosidase H (H) and N-glycosidase F (F) digestion profiles of PrP^C protein in N2a proteins extracts. (D) Control and (Scr) HBE cells were trypsinized and harvested 48 h after transfection and the dead cells were assessed by MTT assays. Data are expressed as mean ± SE (n=4). Values overwritten with stars are significantly different from the control (0 h) (P < 0.05).

